VIBRATIONAL OPTIMIZATION OF A MASS-LOADED STEPPED PLATE

M. Moshrefi-Torbati, C. Simonis de Cloke and A. J. Keane

Department of Mechanical Engineering, University of Southampton, Highfield, Southampton SO17 1BJ, England

In this paper the vibrational characteristics of thin, mass-loaded, stepped plates are investigated. The dimensions of the plates are chosen so that the steps can be thought of as representing the periodically placed stiffeners commonly found in many engineering structures. To achieve this, a classical analytical approach for the analysis of the vibration of a simply supported, stepped plate is first considered. Next, a method for the analysis of such plates carrying concentrated masses is reviewed. The above two analytical methods are then combined to analyse the vibrational behaviour of thin, simply supported and mass-loaded stepped plates. To assess the accuracy of these methods, the resultant frequency responses of the unloaded plate are compared with the Dynamic Stiffness method [1] and those for both the unloaded and mass loaded plates with finite element calculations. For a uniform, mass-loaded plate, there is perfect agreement between the frequency responses obtained from these methods. For the mass-loaded, stepped plate, the agreement is not so complete, the reasons for which are discussed in the paper. The final part of the paper deals with optimisation of the mass positions in order to improve the vibrational behaviour of the plate. In this work, the integral of the frequency response function of the mass-loaded plate over a frequency range containing some 10–15 natural frequencies is regarded as the objective function. The drive and response points are chosen to lie at opposite ends of a plate with high aspect ratio and transverse stiffeners, so that minimizing the frequency response is equivalent to designing vibration isolation characteristics into the plate. The Genetic Algorithm, which is an evolutionary optimization method, is employed to produce the required designs. It is demonstrated that the optimized mass positions significantly improve the vibrational behaviour of the plate.

© 1998 Academic Press Limited

1. INTRODUCTION

An increasingly important area in all fields of engineering is the problem of noise and vibration control. In many engineering structures the main source of noise is vibrations. Structures, such as those of aircraft and ships, often contain many vibrating parts that, despite isolation treatments, excite motions at their mounting points producing such noise. These motions can be large due to the inherently low damping characteristics of the structures and these can propagate large distances through the structure. Commonly, such noise is eradicated by employing heavy viscoelastic damping materials which lead to increases in cost and weight [2]. Another solution that is often adopted is to use vibration isolators between pieces of equipment and their supporting structures. Obviously, isolating large pieces of structures can be difficult and expensive and with some structures, such as the wings on an aircraft, almost impossible.

In recent years, much attention has been focused on active noise control of structures. Using this approach, unwanted vibrations can be cancelled out by the employment of 'anti-noise' to block noise propagation. However, active noise control measures can be

expensive to install and maintain and because of this passive solutions, if achievable, would be preferable. One passive approach that has been extensively studied, mainly for use in aircraft fuselages, makes use of the vibration characteristics exhibited by structures with geometric periodicity. Such structures possess so called 'stop-bands' which are regions of the frequency domain where natural frequencies do not occur and where travelling waves are very rapidly attenuated by constructive reflections [3, 4]. These characteristics become increasingly complex as the nature of the periodicity becomes more complex and also as the structure moves from one, through two, to three dimensional. Furthermore, noise control cannot be based solely on structural periodicity since post-design modifications or lack of accuracy in manufacturing can shift or disrupt the stop bands. If a noise isolation technique is to be of practical use, it must yield robust designs.

Keane [2] has shown that significant noise isolation characteristics can be introduced into structures by modifying their geometries in a controlled manner, using optimization techniques. Moreover, the resultant structures are still functional even at frequencies away from those where the noise control is achieved. The reference notes the improvement in the noise performance of some structures that can be obtained by departing from conventional geometrically uniform designs. This idea is developed further here by its application to plated and stiffened structures.

2. CLASSICAL METHOD

In reference [5], a method for analysing the modes of vibration of simply supported plates with uniform and stepped thicknesses is developed, based on the work of Chopra [6], which was initially applied to a plate with only one change in thickness. The extended results presented there are capable of dealing with the vibration analysis of a multi-stepped plate, especially for high order modes. This is a significant improvement, since the original method is inadequate for high frequency analysis. This is mainly due to the matrix, on which the eigenvalue calculations are based, being ill-conditioned. Furthermore, some boundary conditions that were inappropriately adopted in the original reference were redefined in the later work. In what follows, the steps required to carry out such an analysis are briefly recapitulated.

Consider a multi-stepped plate, simply supported on all sides, as shown in Figure 1. In order to analyse the vibrational behaviour of this plate, it can be divided into parts according to its thickness changes in the longitudinal direction. Each part of the plate, j,
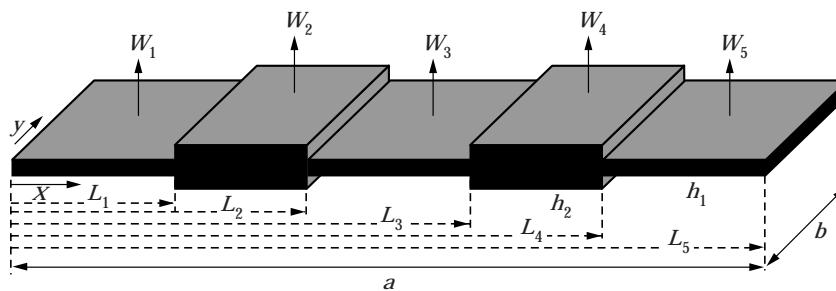

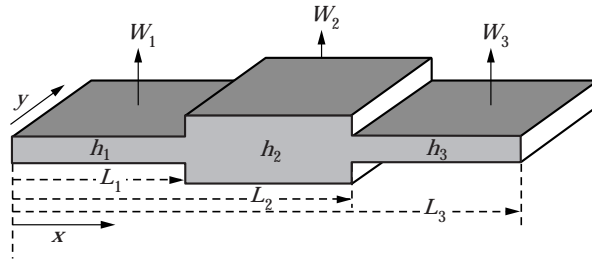Figure 1. A simply-supported stepped plate with four joint lines.

Figure 2. A simply supported stepped plate with two joint lines.

being of uniform thickness, can be represented by the following governing differential equation

$$D_j \, \nabla^4 W_j + \rho t_j \frac{\partial^2 W_j}{\partial t^2} = 0 \tag{1}$$

or assuming harmonic motions for free vibration,

$$(\nabla^4 - k_j^4) W_j = 0 \tag{2}$$

where W_j is the displacement function of the jth part and has the following general solution

$$W_j \, (x, y) = \sum_n \psi_{jn} \, (x) \sin \, (n\pi y/b) \tag{3}$$

where n is the number of nodal lines in the y-direction and $\psi_{jn} \, (x)$ is the shape function in the x-direction which is in turn given by

$$\psi_{jn} \, (x) = A_{jn} \sin \, (\lambda_{1j} \, x) + B_{jn} \cos \, (\lambda_{1j} \, x) + C_{jn} \sinh \, (\lambda_{2j} \, x) + D_{jn} \cosh \, (\lambda_{2j} \, x) \tag{4}$$

where λ_1 and λ_2 are given by

$$\lambda_{1j} = \sqrt{k_j^2 - \alpha^2} \quad \text{and} \quad \lambda_{2j} = \sqrt{k_j^2 + \alpha^2} \quad \text{with} \quad \alpha = n\pi/y. \tag{5}$$

The eigenvalues and mode shapes of the plate can then be found by applying the boundary conditions to (3) for each part and solving for the natural frequencies.

2.1. BOUNDARY CONDITIONS

The shape functions for the first and last plate elements can be reduced by applying the simply supported boundary conditions to them, i.e. displacement and moments at $x = 0$ and $x = a$ are zero. For the middle plates, however, at each joint connecting two plates, four continuity conditions exist. The displacements, slopes, moments and shear forces of the adjacent plates at a joint are the same, and hence, four equations corresponding to each joint line can be established. This implies that for a plate, divided into N parts, there

TABLE 1

Properties of the uniform plate

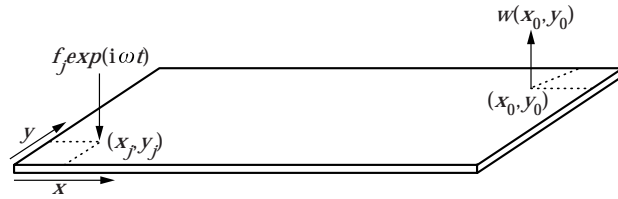|	
$h_1 = h_2 = 0.001$ (m)	Forcing point (x_j, y_j) (m) $= (0.1, 0.1)$
$E = 206.8$ (GPa)	Response point (x_0, y_0) (m) $= (4.9, 0.9)$
$\rho = 2780$ (kg/m^3)	$a = 5$ (m)
$v = 0.29$	$b = 1$ (m)

Figure 3. A simply supported plate excited by a periodic point force.

are $4 \times N$ equations that involve the shape function coefficients of the plates, given by equation (4). The overall equations of the motion of the stepped plate are then given by the following matrix equation

$$[\mathbf{K}(\lambda)]\{\mathbf{C}\} = \{\mathbf{0}\}. \tag{6}$$

The eigenvalues of the vibrating plate are obtained from the frequencies that make the determinant of the matrix $[\mathbf{K}(\lambda)]$ zero. Subsequently, the mode shapes of the plates are obtained by evaluating the relative values of the coefficients A, B, C and D and substituting them back into the shape function (3).

2.2. CALCULATION OF HIGHER MODES

As mentioned earlier, this method usually fails to calculate the high order modes of a stepped plate because of numerical problems. The reason for this is that at high frequencies, the elements of some columns of the $[\mathbf{K}(\lambda)]$ matrix tend to zero and some others tend to large identical values. In either case, the matrix becomes ill-conditioned or singular, leading to difficulties in the numerical analysis of the eigensolutions. To overcome this problem, the shape function (3) can be scaled to accommodate the high frequency behaviour of each plate [5]. Consider the stepped-plate in Figure 2, that contains two joint lines. The shape function of each plate for different frequency ranges can be defined as follows

Plate 1 $(0 < x < L_1)$
for $k^2 > \alpha^2$

$W_1(x, t) =$

$$A_1 \left\{ \sin (\lambda_1 [L_1 - x]) - \tan (\lambda_1 L_1) \cos (\lambda_1 [L_1 - x]) \right\} + C_1 \left\{ \frac{e^{-\lambda_2 (x + L_1)} - e^{\lambda_2 (x - L_1)}}{1 + e^{-2\lambda_2 L_1}} \right\} \tag{7}$$

and for $k^2 < \alpha^2$

$$W_1(x, t) = A_1 \left\{ \frac{e^{-\lambda_1 (x + L_1)} - e^{\lambda_1 (x - L_1)}}{1 + e^{-2\lambda_1 L_1}} \right\} + C_1 \left\{ \frac{e^{-\lambda_2 (x + L_1)} - e^{\lambda_2 (x - L_1)}}{1 + e^{-2\lambda_2 L_1}} \right\}. \tag{8}$$

Note that at the boundaries the effect of the evanescent waves are taken into account explicitly.

Plate 2 $(L_1 < x < L_2)$

At this point, a new parameter is introduced, namely the critical frequency ω_{crit} above which the matrix $[\mathbf{K}(\lambda)]$ in expression (6) becomes ill-conditioned (typically when the differences between the exponential functions lie beyond the numerical accuracy of the computer used). Therefore, in addition to the frequency conditions applied to plate 1, the

shape function is now also defined for ω_{crit}. For $k^2 > \alpha^2$ and $\lambda_2 (L_2 - L_1) < \omega_{crit}$ this gives

$$W_2 (x, t) = A_2 \sin (\lambda_1 [x - L_1]) + B_2 \cos (\lambda_1 [x - L_1]) + C_2\, e^{-\lambda_2 (x - L_1)} + D_2\, e^{\lambda_2 (x - L_1)} \quad (9)$$

and for $k^2 > \alpha^2$ and $\lambda_2 (L_2 - L_1) > \omega_{crit}$

$$W_2 (x, t) = A_2 \sin (\lambda_1 [x - L_1]) + B_2 \cos (\lambda_1 [x - L_1]) + C_2\, e^{-\lambda_2 (x - L_1)} + D_2\, e^{\lambda_2 (L_2 - x)}. \quad (10)$$

In both of the above cases, for the condition when $k^2 < \alpha^2$, the shape function is obtained by replacing the periodic functions (sin and cos) with hyperbolic ones (i.e. sinh and cosh).
Plate 3 $(L_1 < x < L_2)$
for $k^2 > \alpha^2$

$$W_3 (x, t) = A_3 \{\sin (\lambda_1 [x - L_2]) - \tan (\lambda_1 [L - L_2]) \cos (\lambda_1 [x - L_2])\}$$
$$+ C_3 \{\sinh (\lambda_2 [x - L_2]) - \tanh (\lambda_2 [L - L_2]) \cosh (\lambda_2 [x - L_2])\} \quad (11)$$

and again, for $k^2 < \alpha^2$, the periodic functions are replaced by hyperbolic functions.

3. THE OPTIMIZER

Optimization problems of the sort posed here are characterised by having many variables, highly non-linear relationships between the variables and the objective function, and an objective function that has many peaks and troughs. Moreover, any one configuration is time consuming to evaluate. In short they are difficult to deal with. The
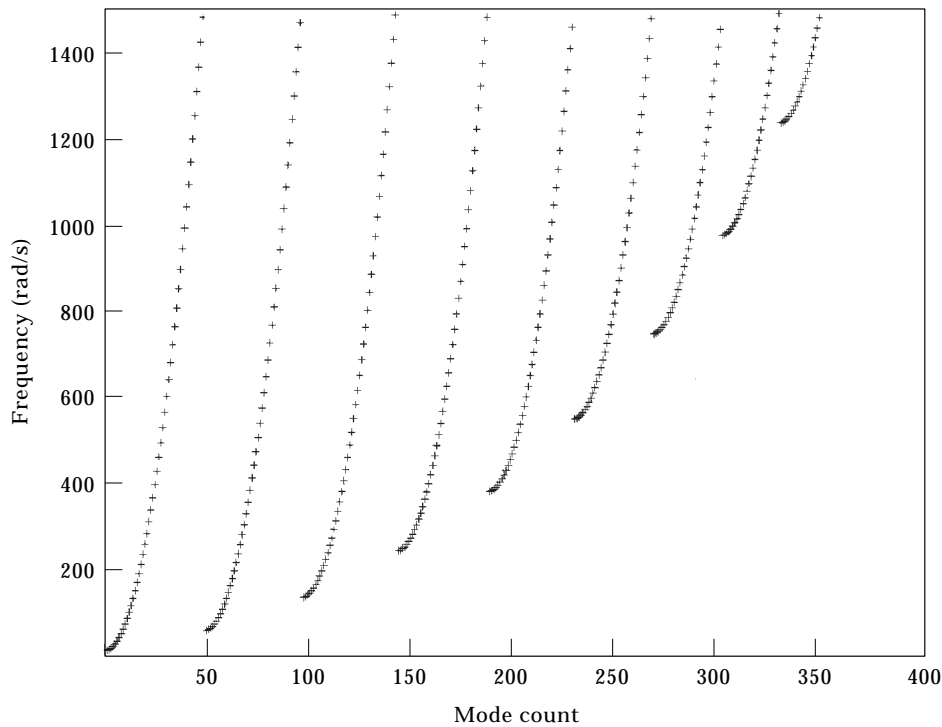

Figure 4. Natural frequencies of the first 50 odd modes corresponding to $n = 1$–9, uniform plate.

TABLE 2

Number of modes lying in the frequency range 0–1000 *rad/s*

Nodal line (n)	1	2	3	4	5	6	7	8
Mode (m)	40	39	37	35	31	27	20	5

search for methods that can cope with such problems has lead to the subject of evolutionary computation. Techniques in this field are characterised by a stochastic approach to the search for improved solutions, guided by some kind of evolutionary control strategy. These are three main methods in use: (i) simulated annealing [7], where the control strategy is based on an understanding of the kinetics of solidifying crystals; (ii) genetic algorithms [8], where the methods of Darwinian evolution are applied to the selection of 'fitter' designs and (iii) evolutionary programming [9], which is a more heuristic approach to the problem but which has an increasing number of adherents.

The General Algorithm (GA) used here is fairly typical of those discussed in the well known book by Goldberg [8] but encompasses a number of new ideas that are particularly suited to engineering design problems [10, 11]. Such methods work by maintaining a pool or population of competing designs which are combined to find improved solutions. In their basic form, each member of the population is represented by a binary string that encodes the variables characterising the design. The search progresses by manipulating the strings in the pool to provide new generations of designs, hopefully with better properties
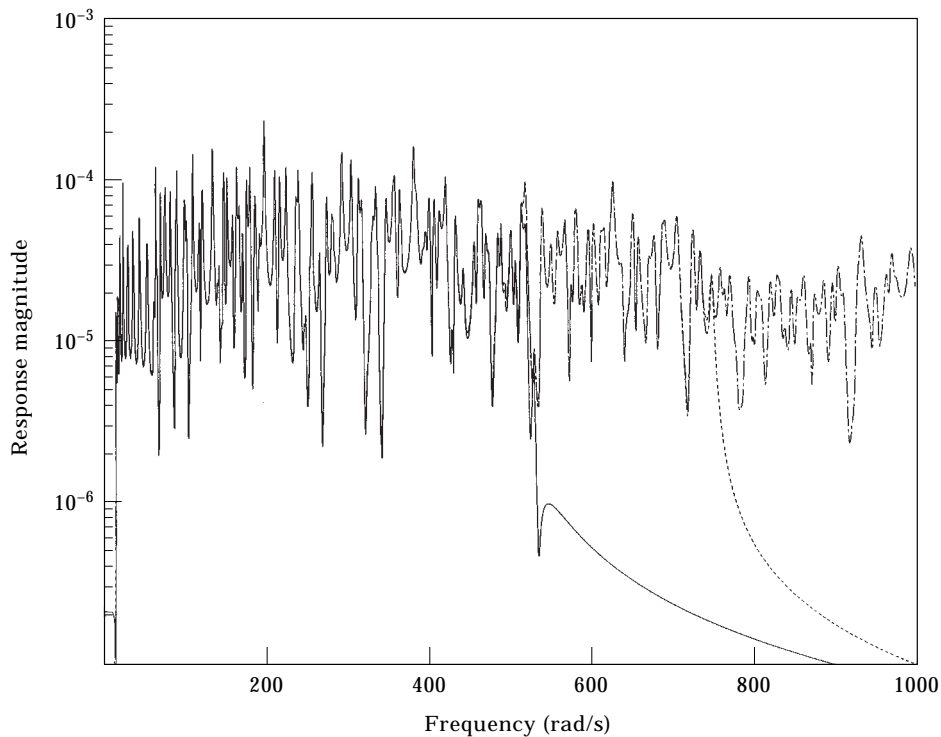

Figure 5. Response (deflection in m per unit force in N) of the uniform plate for various modal summation widths: —— 0–500 rad/s; − − − 0–750 rad/s; − · − · − 0–1000 rad/s.

on average than their predecessors. The processes that are used to seek these improved designs are set-up to mimic those of natural selection: hence the method's name. The most commonly used operations are currently: (i) selection according to fitness, i.e. the most promising designs are given a bigger share of the next generation; (ii) crossover, where portions of two good designs, chosen at random, are used to form a new design, i.e. two parents 'breed' an 'offspring'; (iii) inversion, whereby the genetic encoding of a design is modified so that subsequent crossover operations affect different aspects of the design and (iv) mutation, where small but random changes are arbitrarily introduced into a design. In addition, the number of generations and their sizes must be chosen, as must a method for dealing with constraints (usually by application of a penalty function).

   The algorithm used here works with 12 bit binary encoding. It uses an elitist survival strategy which ensures that the best of each generation always enters the next generation and has optional niche forming to prevent dominance by a few moderately successful designs preventing wide ranging searches. Two penalty functions are available to deal with constraints. The main parameters used to control the method may be summarised as follows: the number of generations allowed (default 10), the population size or number of trials used per generation which is therefore inversely related to the number of generations given a fixed number of trials in total (default 100), the proportion of the population that survive to the next generation (default 0·8), the proportion of the surviving population that are allowed to breed (default 0·8), the proportion of this population that have their genetic material re-ordered (default 0·5), the proportion of the new generation's genetic material that is randomly changed (default 0·005); a proportionality flag, which
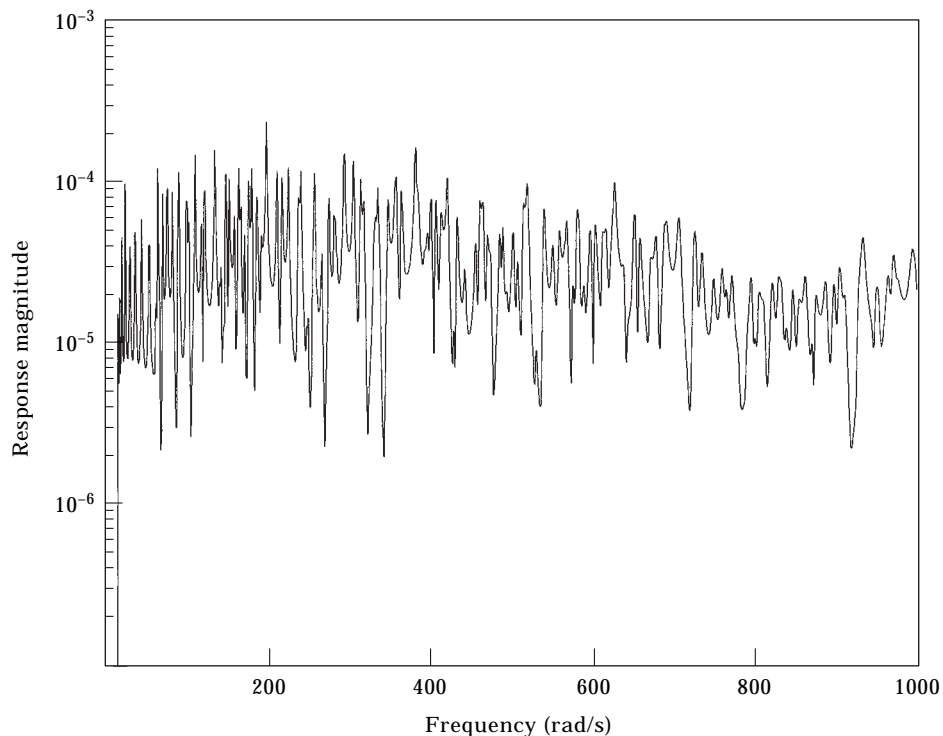

Figure 6. Response (deflection in m per unit force in N) of the uniform plate compared with results from the dynamic stiffness method: —— modified Chopra method; – – – dynamic stiffness method (curves virtually identical).
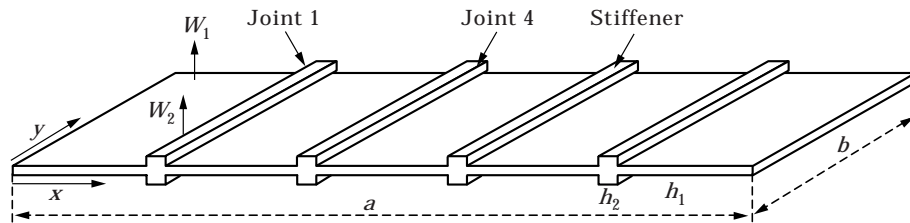
Figure 7. A simply supported stepped plate with eight joint lines.

selects whether the new generation is biased in favour of the most successful members of the previous generation or alternatively if all the best survivors are propagated equally (default TRUE), and the penalty function choice.

When using the GA to explore large design spaces with many variables, it has also been found that the method must be prevented from being dominated by a few moderately good designs which prevent further innovation. A number of methods have been proposed to deal with this problem; that used here is based on MacQueen's Adaptive KMEAN algorithm [12] which has recently been applied with some success to multi-peak problems [13]. This algorithm subdivides the population into clusters that have similar properties. The members of each cluster are then penalized according to how many members the cluster has and how far it lies from the cluster centre. It also, optionally, restricts the crossover process that forms the heart of the GA, so that large successful clusters mix solely with themselves. This aids convergence of the method, since radical new ideas are prevented from contaminating such sub-pools.

In addition, the implementation of the GA used here allows the solution of individual members of the population to be run in parallel if a multiple processor computer is available.

4. EXAMPLE CALCULATIONS

Perhaps the best way to examine the performance of this method is to apply it to a uniform flat plate modelled by several equal thickness sections. In this way, all the boundary conditions are employed except those related to thickness ratio between adjacent plates and the exact results are easy to establish. Consider, a 4-joint plate, as already shown in Figure 1, but now with the same properties for each element, as per Table 1.

Next, for comparison, consider a single lightly damped uniform plate with pairs of opposite sides that are simply supported, being excited on (x_j, y_j), by a harmonic point force $f_j \exp(i\omega t)$, as depicted in Figure 3. The deflection w of the plate at x_0, y_0 due to the point force is given by

$$w(x_0, y_0\,;\,\omega) = f_j\,g(x_j, y_j, x_0, y_0\,;\,\omega) \tag{12}$$

where

$$g(x_j, y_j, x_0, y_0\,;\,\omega) = \sum_{m=1}\sum_{n=1}\frac{\psi_{mn}(x_j, y_j)\psi_{mn}(x_0, y_0)}{b_{mn}(\omega_{mn}^2 - \omega^2 + i2\eta\omega\omega_{mn})} \tag{13}$$

is the Green Function [14] for any two-dimensional system, in terms of its uncoupled modes. In this case, the eigenfunctions are given simply by

$$\psi_{mn}(x_j, y_j) = \sin(m\pi x/a)\sin(n\pi y/b) \tag{14}$$

TABLE 3

Dimensions of the stepped plate

$h_1 = 0·001$ (m)	Forcing point $(x_j, y_j) = (0·1, 0·1)$ (m)
$h_2 = 0·002$ (m)	Response point $(x_0, y_0) = (4·9, 0·9)$ (m)
8-Joints positioned at	$a = 5$ (m)
(0·9, 1·0, 1·9, 2·0, 2·9, 3·0, 3·9, 4·0) (m)	$b = 1$ (m)

and the eigenvalues by

$$\omega_{mn} = \sqrt{D/\rho h} \, \{(m\pi/a)^2 + (n\pi/b)^2\} \tag{15}$$

while the orthogonality constant for mass normalized modes is $b_{mn} = \rho hab/4$. Comparison with this simple theory serves to illustrate a number of aspects of the model used.

4.1. NUMBER OF MODES REQUIRED FOR HARMONIC ANALYSIS

As noted in the previous sub-section the harmonic response of a plate is found here by use of Green functions based on two infinite summations over the plate's modes. However, to obtain the response in practical calculations, one has to choose a finite number of modes that contribute towards the response at any frequency of interest. Apart from obvious concerns regarding accuracy, there is another important consideration here. Since optimization is the ultimate objective of this work, speed of calculation is important. The calculation of mode shapes and their natural frequencies, particularly for higher modes,
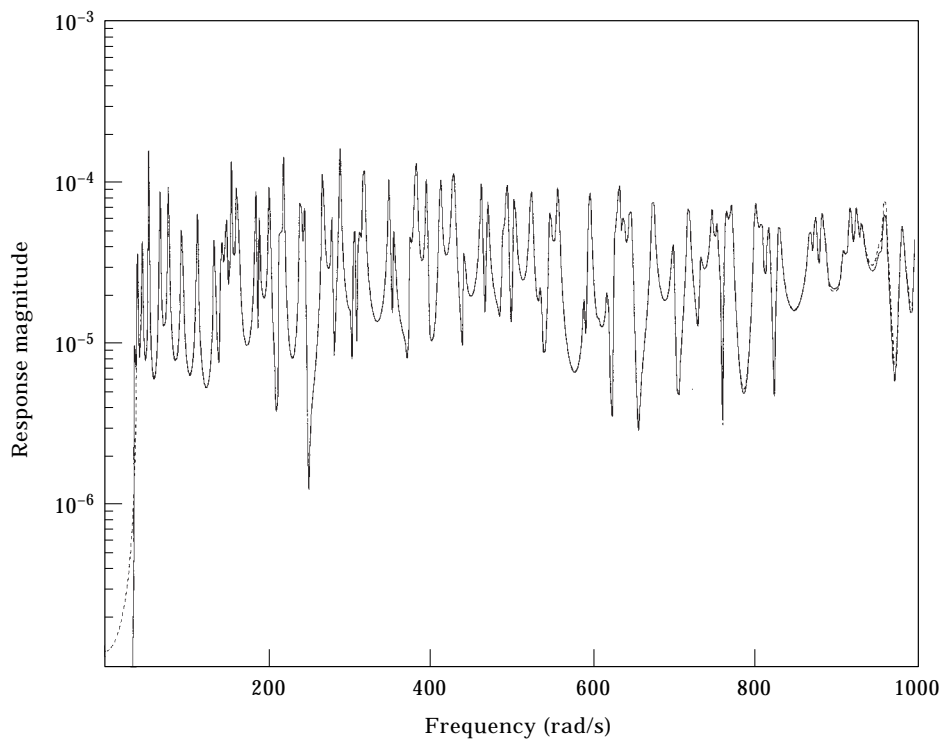

Figure 8. Response (deflection in m per unit force in N) of the stepped plate compared with results from the dynamic stiffness method; key as per Figure 6 (curves virtually identical).
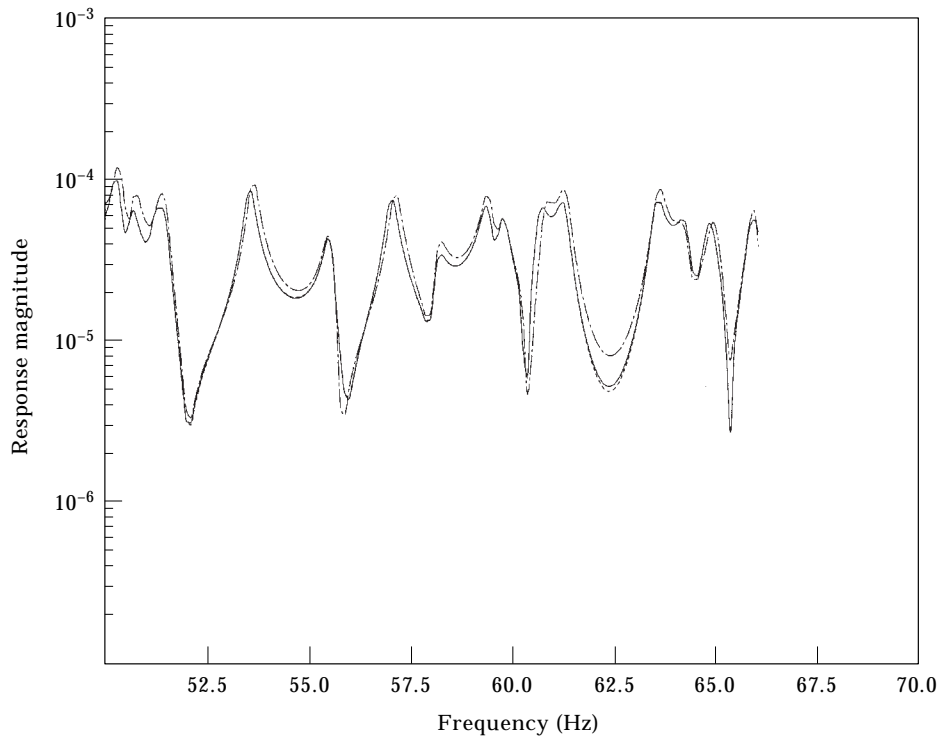
Figure 9. Response (deflection in m per unit force in N) of the stepped plate compared with results from the dynamic stiffness and finite element methods for the frequency range of 50–70 Hz: —— modified Chopra method; – – – dynamic stiffness method; – · – · – finite element method (modified Chopra and dynamic stiffness methods virtually identical).

is somewhat time consuming. Therefore, using modes that do not significantly contribute towards the response within the frequency range of interest, is inefficient. Hence, one has to estimate the minimum number of modes that are required for response calculations. Figure 4 illustrates the variation of natural frequencies of each of the first 50 odd modes corresponding to $n = 1$–9. As can be readily seen, as the nodal lines increase in number, the frequencies of the modes increases almost linearly. So, if for the example in hand, the frequency range of interest were between 0 and 1000 rad/s, then the number of modes for each nodal line lying at or below this frequency would be as given in Table 2.

Figure 5 then shows the response of the uniform plate for various number of modes, covering frequency ranges of 0–500, 0–750 and 0–1000 rad/s. It is clear that apart from the small differences near zero, the three responses are almost identical up to the cut off points of the 0–500 and 0–750 curves, after which they drop to zero, as expected.

It is also worth noting that, as far as speed of calculation is concerned, there is one further piece of information that can be extracted from this figure. In the method employed here, for each nodal configuration a search has to be carried out to find its natural frequencies. Again, time is wasted if this search is carried out over the entire frequency range of interest. Setting the lower search frequency close to that of the first mode for each nodal line, saves time and speeds up this calculation. The above approach has been used in obtaining the responses of all the cases presented here. The
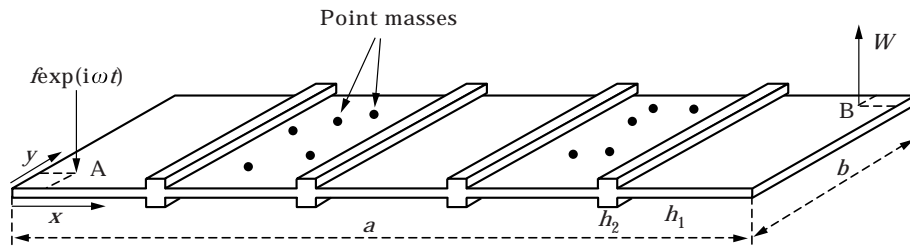
Figure 10. A simply supported mass-loaded, stepped plate with eight joint lines.

response of the uniform plate depicted in Figure 3, is plotted in Figure 6 for the frequency range of 0–1000 rad/s, together with results for the dynamic stiffness method [1]. It can be seen from the figure that there is a perfect agreement between the various methods as the curves are indistinguishable over most of the range of frequencies.

4.2. HARMONIC RESPONSE OF A STEPPED PLATE

To demonstrate the effectiveness of this method when applied to a stepped plate, a simply supported steel plate with four stiffeners is considered next (see Figure 7). The dimensions and properties of the plate are given in Table 3. The stiffener to plate thickness ratio is 2 : 1 and the plate is divided into nine parts (five plates and four stiffeners, reminiscent of a typical plated and stiffened structure). The natural frequencies and forced response of the plate have been calculated and the results are compared here with the dynamic stiffness and finite element methods. The finite element vibration analysis was
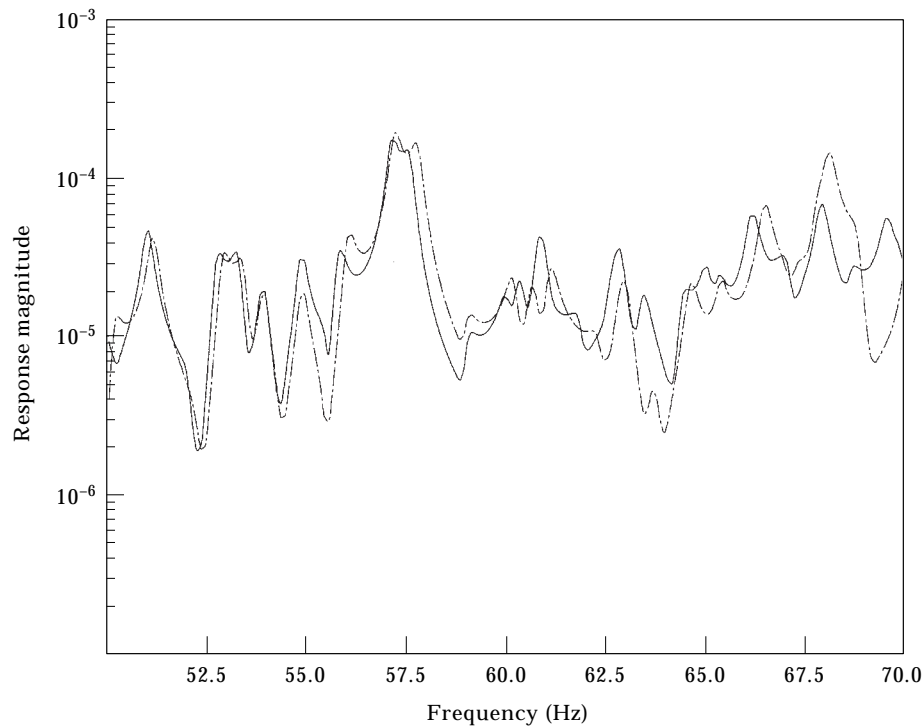

Figure 11. Response (deflection in m per unit force in N) of the mass-loaded, uniform plate, compared with results from the finite element method (0·5 kg masses): —— FDF method; – · – · – finite element method.
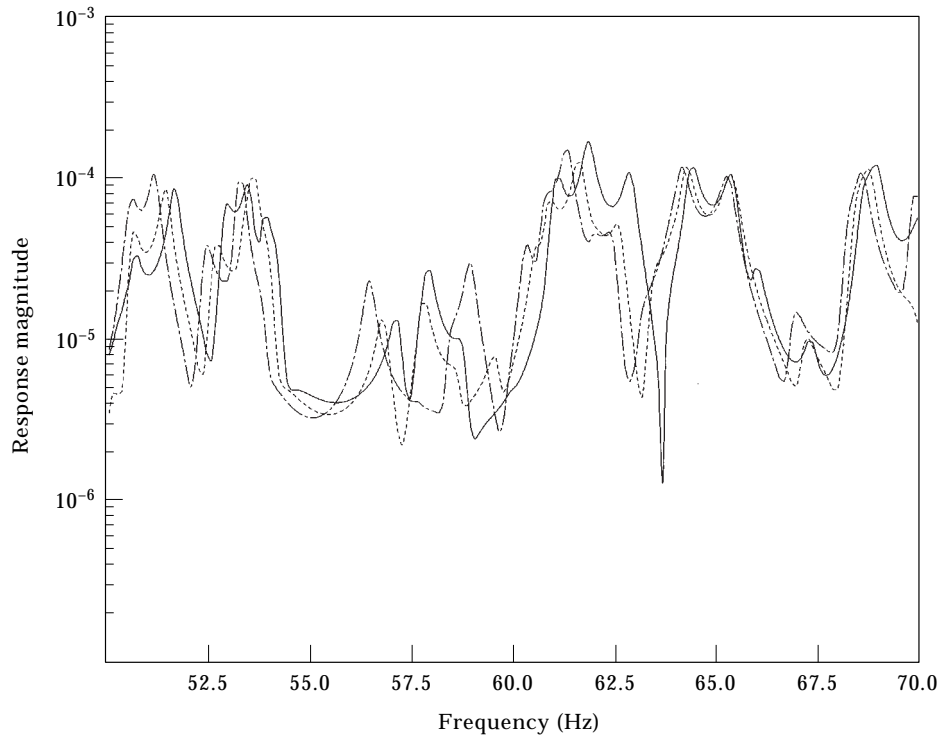
Figure 12. Response (deflection in m per unit force in N) of the mass-loaded, stepped plate for various modal summation widths: ——— 0–750 rad/s; – – – 0–1000 rad/s; – · – · – 0–1500 rad/s.

performed using IDEAS [15] which is a widely used commercial package. The main part of the grid was formed with some 500 four noded-quadrilateral elements using Kirchhoff thin plate theory. The response of the stepped plate is compared with the dynamic stiffness method in Figure 8 for the frequency range of 1–500 rad/s. It can be seen that, apart from the very low frequency values (i.e. <20 rad/s) there is almost a perfect agreement between the two curves. See also Figure 9 where comparison is made for the reduced frequency range of 314·2–439·8 rad/s (50–70 Hz), together with the results of the finite element method (this frequency range is adopted later for the purposes of optimization). The graph shows very good agreement between the three methods with a maximum error of about 2·3% occurring at around 63 Hz.

5. HARMONIC RESPONSE OF A MASS-LOADED STEPPED PLATE

As mentioned earlier, the objective of this work is to explore the possibility of using point masses to modify the vibrational behaviour of stiffened plates. Such designs could subsequently be used in passive noise control, which is the ultimate aim of the current project. McMillan and Keane [16] investigated three different approaches to the analysis of mass-loaded plates and compared their results with the finite element method. Based on their results, the most appropriate method for this work is what they termed the Frequency Dependent Forces (FDF) method. In this method, each point mass is treated as a frequency dependent force from which the frequency response of the plate can be determined in terms of the unloaded plate Green function. In what follows, the FDF method is briefly outlined.

5.1. THE FREQUENCY DEPENDENT FORCES (FDF) METHOD

The partial differential equation for forced motion of the plate can generally be written as

$$D\nabla^4 w + \rho h \frac{\partial^2 w}{\partial t^2} = F(x, y, t) \qquad (16)$$

where all the symbols have their usual meanings and $F(x, y, t)$ is the sum of all forces applied to the plate and includes both (a) a real force f_j applied at (x_j, y_j), which can be expressed as: $F(x, y, t) = f_j \delta(x - x_j)\delta(y - y_j) e^{i\omega t}$ and (b) all forces associated with the loading due to the point masses. Earlier the harmonic response of a uniform plate to a point force was noted, see equations (12) and (13). Now, if there are l masses attached to the plate with positions (x_k, y_k) then each mass, M_k, provides a point force on the plate of

$$f_k(x, y) = -M_k \frac{\partial^2 w}{\partial t^2} = M_k \omega^2 w(x_k, y_k). \qquad (17)$$

The deflection of the plate at any point (x_0, y_0) due to the applied force f_j and those due to the l masses is thus given by

$$w(x_0, y_0, \omega) = f_j g(x_j, y_j, x_0, y_0 ; \omega) + \sum_{k=1}^{l} f_k g(x_k, y_k, x_0, y_0 ; \omega). \qquad (18)$$
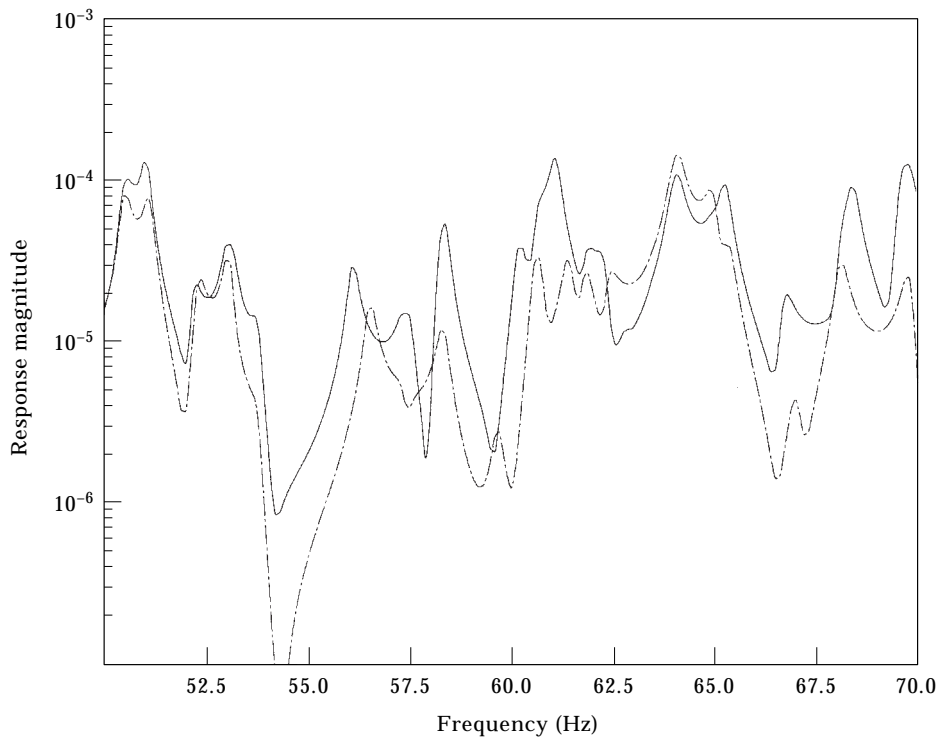

Figure 13. Response (deflection in m per unit force in N) of the mass-loaded, stepped plate compared with results from the finite element method (0·5 kg masses); key as per Figure 11.

TABLE 4

Original and optimized objective functions for various mass numbers and mass positions

Number of masses	Original obj. function	Optimized obj. function	Ratio orig/optim.	Ratio optim/ unloaded*
1(L)	0.3559×10^{-4}	0.9986×10^{-5}	3·56	3·39
1(R)	0.2473×10^{-4}	0.1335×10^{-5}	1·85	2·53
2(L)	0.1819×10^{-4}	0.4377×10^{-5}	4·16	7·73
2(R)	0.2436×10^{-4}	0.5779×10^{-5}	4·22	5·85
2(LR)	0.4304×10^{-4}	0.3235×10^{-5}	13·30	10·46
5(L)	0.1754×10^{-4}	0.1991×10^{-5}	8·81	16·99
5(R)	0.3887×10^{-4}	0.2481×10^{-5}	15·67	13·64
10(LR)	0.3061×10^{-4}	0.8864×10^{-5}	34·53	38·17
20(LR)	0.3060×10^{-4}	0.1487×10^{-5}	20·58	22·75

L: all masses on the 2nd bay, R: all masses on the 4th bay, LR: half the number of masses on the 2nd and half on the 4th bay, see Figure 10.

* The objective function for the unloaded plate is 0.3383×10^{-4}.

Now, for each of the l masses positioned on the plate, by using equation (17), l equations of the form

$$f_k = M_k \, \omega^2 \left\{ f_j \, g(x_j, y_j, x_0, y_0 \, ; \omega) + \sum_{k=1}^{l} f_k \, g(x_k, y_k, x_0, y_0 \, ; \omega) \right\} \qquad (19)$$
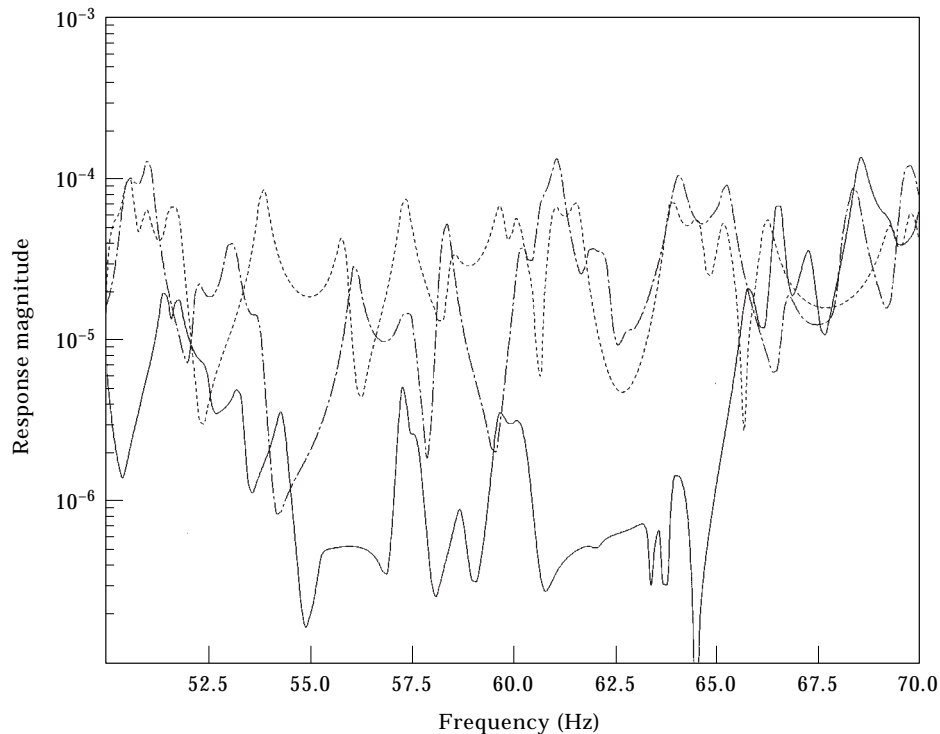

Figure 14. Response (deflection in m per unit force in N) of the optimized mass-loaded, stepped plate, compared with that for the randomly mass-loaded plate and the unloaded plate (ten 0·5 kg masses): —— optimized mass-loaded plate; – – – randomly mass-loaded plate; – · – · – unloaded plate.

are obtained. These simultaneous equations can then be solved for the l unknown frequency dependent forces f_k. The deflection of the plate at any point (x_0, y_0) can subsequently be found by using equation (18). However, in the original reference a uniform thickness plate was considered for which the Green function is well known, whereas the plate being studied here is stepped. Therefore, the Green function has to be obtained from the modified Chopra method already discussed in Section 2. In doing so, the mode shapes in equation (13) have to be normalized for the stepped plate and as a result, the coefficients b_{mn} in the Green function are then given by

$$b_{mn} = \sum_{i=1}^{N} \rho h_i \int_0^b \int_{L_{i-1}}^{L_i} \psi_{mn}^2(x, y) \, \mathrm{d}x \, \mathrm{d}y = \rho b/2 \sum_{i=1}^{N} h_i \int_{L_{i-1}}^{L_i} \psi_{mn}^2(x) \, \mathrm{d}x. \qquad (20)$$

Note that since the plate is uniform in the y-direction, the integral of the shape function squared, between zero and width b is simply $b/2$.

5.2. NUMBER OF MODES REQUIRED FOR HARMONIC ANALYSIS OF A MASS-LOADED PLATE

It was noted earlier that in calculating the harmonic response of a plate by use of the Green function summation, only a finite number of modes that contribute towards the response need be used. It was shown that in order to reduce computation time, it is possible to find the minimum number of modes required for accurate evaluation of the response and that accurate results can be obtained by summing over those modes that fall within the frequency range of interest. Obviously, by adding point masses, the behaviour of the plate is altered and the above conclusion cannot be applied directly. As was discussed in
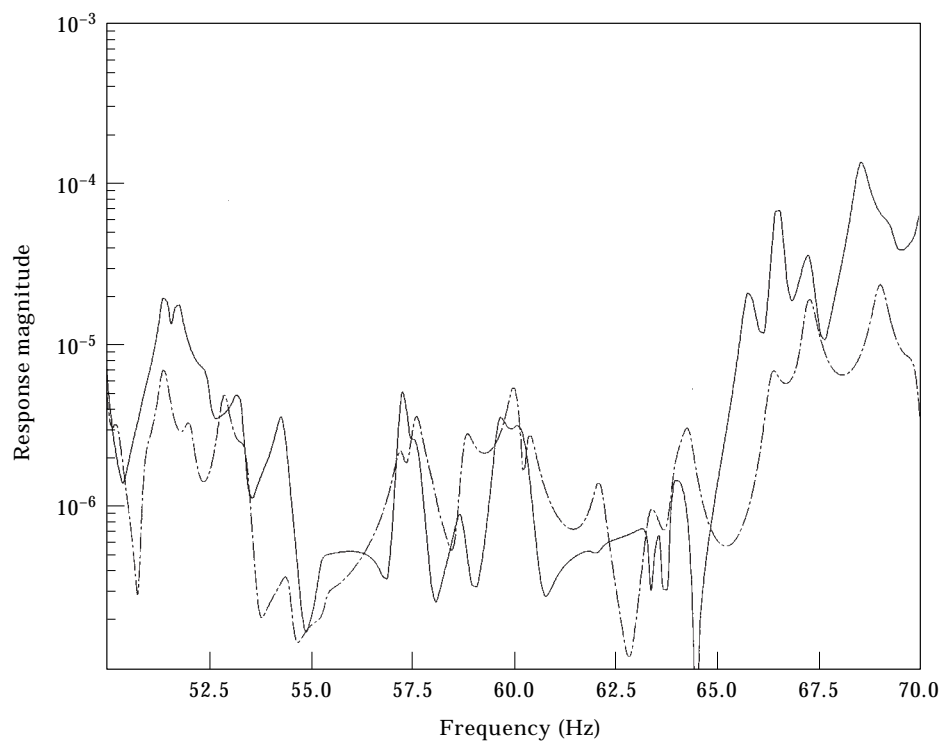

Figure 15. Response (deflection in m per unit force in N) of the optimized mass-loaded, stepped plate, compared with results from the finite element method (ten 0·5 kg masses); key as per Figure 11.
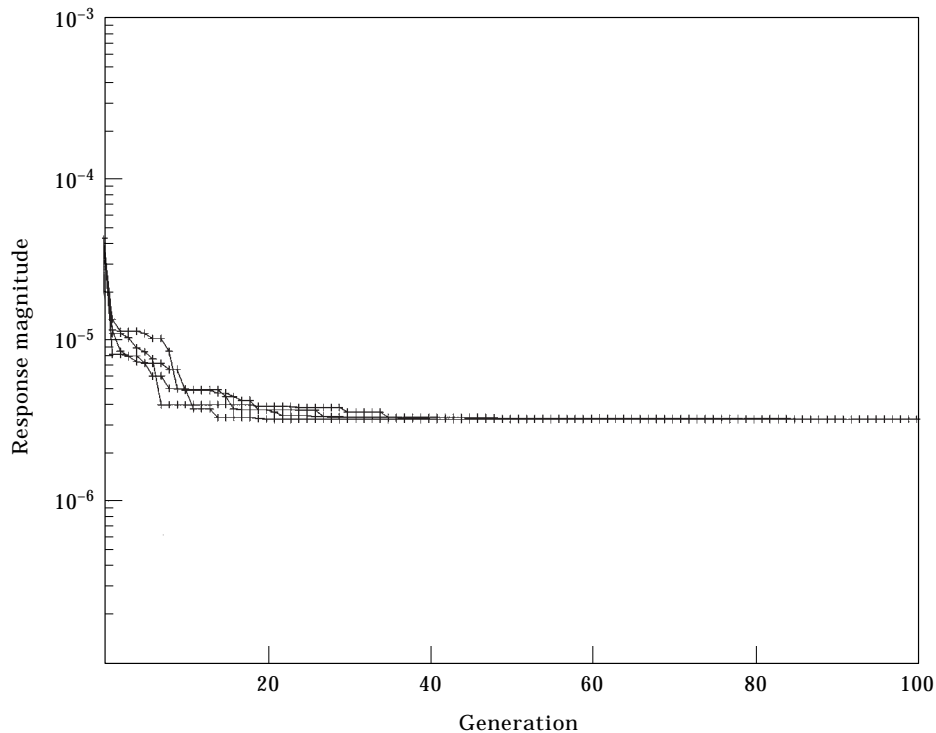
Figure 16. Objective function variations (deflection in m per unit force in N) for the stepped plate carrying two 2·5 kg point masses [i.e. 2(LR)], obtained for four independent runs with different random number sequences.

the last section, the response of a mass-loaded plate is carried out here through the FDF method which uses the mode shapes and natural frequencies of the unloaded plate. Hence, information is not used for the mode shapes and natural frequencies of the combined mass-loaded plate and consequently, the minimum number of modes for response calculations has to be found empirically. Various examples with different mode combinations were carried out and the responses compared with FE models. It was then concluded that in order to obtain a reasonably accurate response of the mass-loaded plate, modes that fall within a frequency range from zero to three times that of the range of interest should be used. In the following sections this criterion is used when calculating the response of the mass-loaded stepped plate.

5.3. NUMERICAL EXAMPLE FOR MASS-LOADED PLATES

In this section the uniform and stepped plates analysed earlier are employed again but now 10 point masses are randomly positioned on the two plate elements that are bounded within $x = 1·0$–$1·9$ and $x = 3·0$–$3·9$ m (see Figure 10). The overall value of the point masses is taken to be about 10% of the plate's weight. The combined revised Chopra and FDF methods are used to calculate the response of the mass-loaded stepped plate. The harmonic responses of the combined system are calculated for the arbitrary frequency range of 50–70 Hz and the results compared with those from the finite element (FE) method. The FE model employs a 10×50 mesh, each element having dimensions of 10×10 cm. Figure 11 shows the harmonic response of the mass-loaded, uniform plate together with the FE results. It can be seen that there is a good agreement between the two curves for most frequencies.

At this point, it is worth examining the effect of modal summation width on the response of the mass-loaded plate. Figure 12 shows the response of the mass-loaded plate for various modal summations (cf. Figure 5). The figure shows that improved results are obtained by adding more modes, as expected. However, as will be discussed later, in this work the area under the response curve is the main goal, as this measures energy transfer and the change in this quantity is not very significant. Finally, the harmonic response of the mass-loaded, stepped plate is plotted in Figure 13, together with the FE results. As expected the agreement between the curves is not as good as for the uniform plate. This is mainly because in the FDF method, any error due to inaccuracy in the estimation of the mode shapes accumulates in the calculations of the mass-loaded response, as the Green function is used l^2 times in solving the simultaneous equations (19).

6. OPTIMIZATION OF MASS POSITIONS

Having obtained the harmonic response of a mass-loaded, stepped plate, the next consideration is the search for the best mass positions to obtain the desired response. The idea here being to apply minor changes to the structure, but which are big enough to modify its frequency response. The changes are targeted towards the suppression of vibrations within a given frequency band, reducing the overall vibrational energy transfer of the structure. Here again, the long rectangular stepped plate carrying a series of identical point masses is considered, already illustrated in Figure 10.

The plate is excited by a unit harmonic point force at point A on the plate and the response is measured at point B. The integral of the frequency response over the frequency
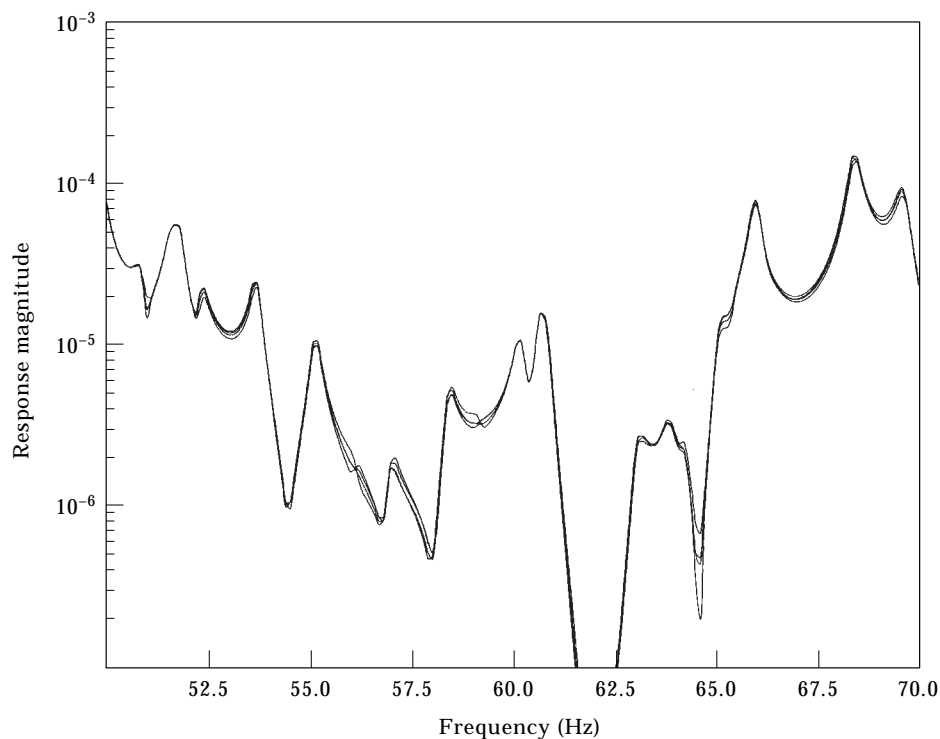

Figure 17. Response (deflection in m per unit force in N) of the stepped plate carrying two 2·5 kg point masses [i.e. 2(LR)], obtained for four independent runs with different random number sequences.
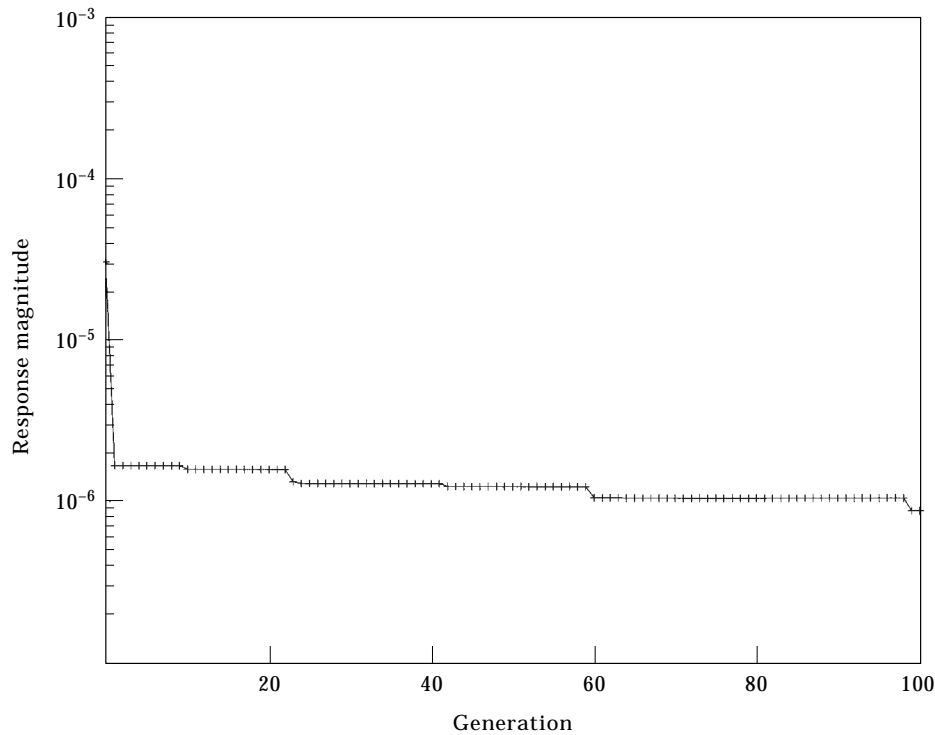
Figure 18. Objective function variation (deflection in m per unit force in N) for the stepped plate, carrying ten 0·5 kg masses.

range of 55–65 Hz is regarded as the *objective function* which is to be minimized. As far as the optimization process is concerned, due to the large number of variables present in this problem, using traditional slope descent based methods would be very time consuming. However, there are a number of recently developed evolutionary techniques that are ideal for dealing with problems containing large search spaces [2]. One advantage of these techniques over traditional slope based methods is that their convergence rates are typically less rapidly deteriorated by increases in the number of variables. In this work, the GA described earlier is employed to produce the desired design.

7. RESULTS AND DISCUSSION

For this study the total mass of the point masses is taken to be 5 kg in all the cases presented. Optimization runs were carried out on the plate when loaded with 1, 2, 5, 10 and 20 randomly placed masses. In all cases the point masses were constrained to lie within the second and fourth bays of the plate since it was considered that such positions would effectively break up any travelling waves tuned to the periodic nature of the structure, without the need to search over the whole domain for suitable positions. Here 25 000 GA iterations were used with a population size of 250 and the values of the best objective function recorded for each population. Table 4 compares the optimized objective function (i.e. integral of the forced response of the plate between 55 and 65 Hz) after 25 000 iterations for each case with the objective function evaluated for the original, random, mass positions and also for the stepped plate without masses. From the table it is clear that the best result after 25 000 iterations is obtained for the plate carrying 10 masses although it

is obvious that a fully optimized 20 mass arrangement should be at least as good as the best 10 mass design. Clearly, 25 000 iterations is not enough to ensure convergence for a case with so many variables. Even so, the 20 mass design represents almost eight times as much computational effort as the 10 mass case since the bulk of the effort involved in studying the performance of such designs lies in the solution of the simultaneous equations inherent in the FDF analysis. (In fact, a further very extensive search over some 400 000 iterations for the 20 mass case results in an objective function of 0.7228×10^{-6}, i.e. now significantly better than for the 10 mass case but at enormous computational cost.)

The response of the plate with 10 masses placed at these optimized positions is plotted in Figure 14, together with that for 10 randomly positioned masses and also the unloaded plate. The figure demonstrates a clear drop in the plate's response within the frequency range of 55–65 Hz, the maximum of which is about 3 decades, occurring at around 64 Hz. The response of this optimized design may be validated by comparing against a finite element analysis for these mass positions (see Figure 15). The figure shows that, although there are differences between the responses calculated by these two methods the overall improvements in the design are preserved and the areas under the curves very similar.

Having noted that the 20 mass design achieved by optimization with 25 000 iterations cannot be fully converged, attention is next turned to the stochastic nature of the optimization method used. In order to gain confidence in the final result of a stochastic method applied to a problem with many possible solutions, it is useful to employ runs with different random number sequences [2]. Here, this confidence test is applied to the case of one point mass placed on each of the 2nd and 4th bays of the stepped plate (computational limits prevented it being applied to the cases with more masses). Four
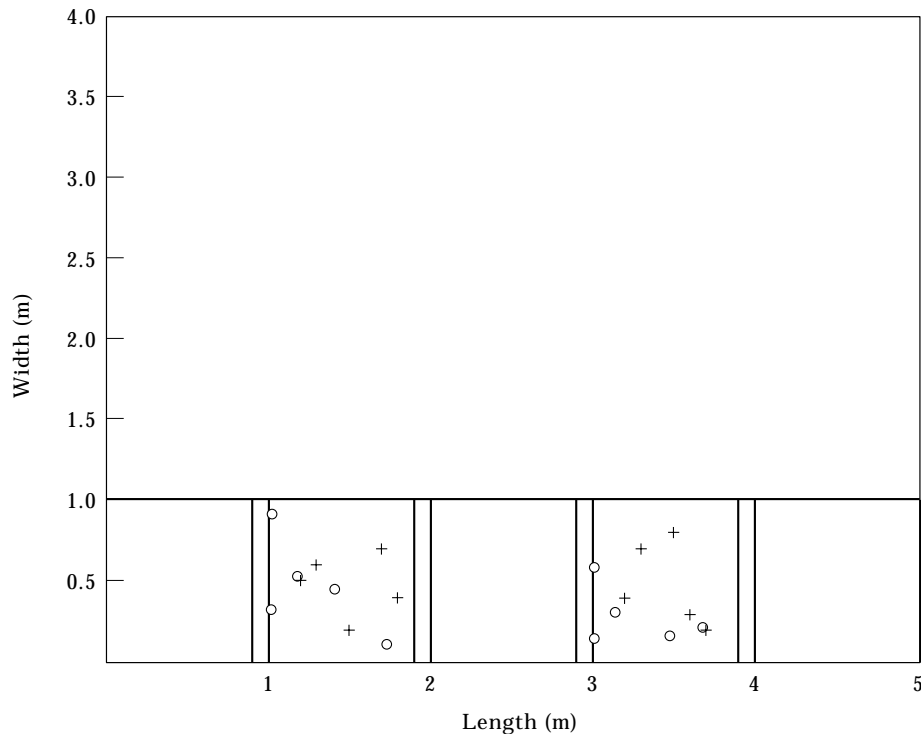

Figure 19. Optimized mass positions after spatial averaging (○) together with the original, random positions (+).
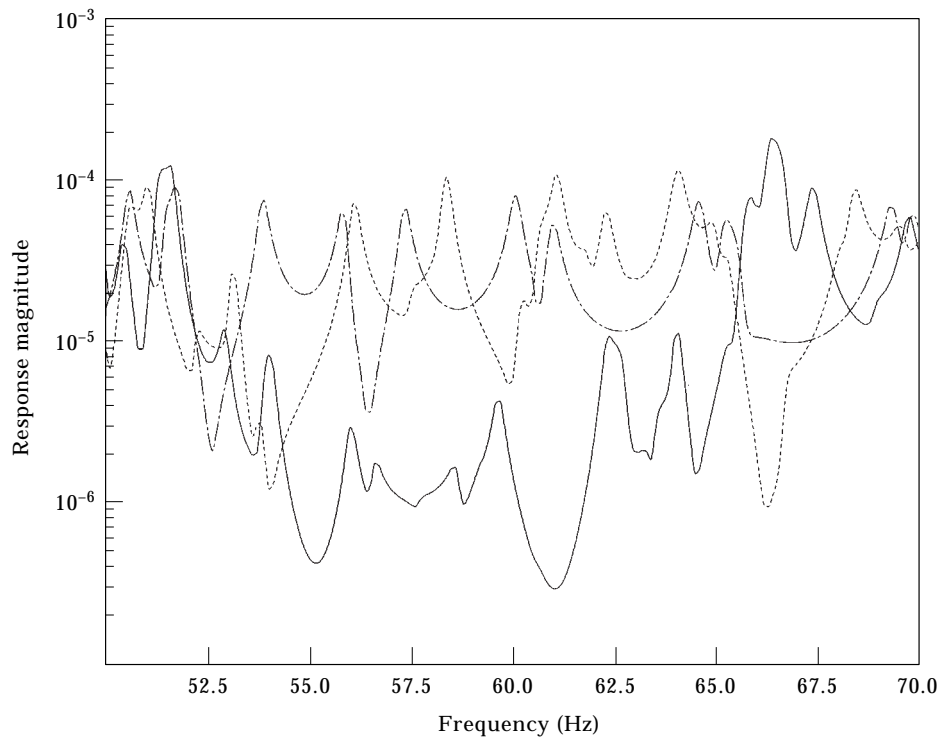
Figure 20. Response (deflection in m per unit force in N) of the spatially averaged and optimized mass-loaded, stepped plate, compared with that for the randomly mass-loaded plate and the unloaded plate (ten 0·5 kg masses); key as per Figure 14.

independent runs of 25 000 iterations were carried out and the values of the best objective functions for each of the generations recorded (see Figure 16). The resonse of the mass-loaded plate for the final optimized mass positions, corresponding to the four runs, are depicted in Figure 17. These figures clearly demonstrate the robustness of the GA method used, with all four cases converging towards the same final optimized result for this more limited problem. A plot of the objective function against number of search iterations for the 10 mass case discussed earlier indicates that this design is probably not converged, however (see Figure 18). With further computational effort it would no doubt be possible to obtain even greater reductions in energy transmission for this case, although it is by no means clear how much further effort would be warranted given the large improvements already obtained.

7.1. SPATIAL AVERAGING

Having found sets of reasonably well optimized mass positions the final area to be considered concerns the performance of the optimized designs in practice. When dealing with structural dynamics it is very difficult to build real structures that are identical to the ones used in simulations. The vibrational behaviour of real structures commonly differs markedly from the inevitably idealized models used for calculations, particularly in regards to the values of individual natural frequencies and the mode shapes that they yield. Therefore, a highly optimized computational solution to a problem will not necessarily produce the modelled results in practice and consequently, predicted reductions in the objective function may not be obtained. It has been found that averaging spatially over
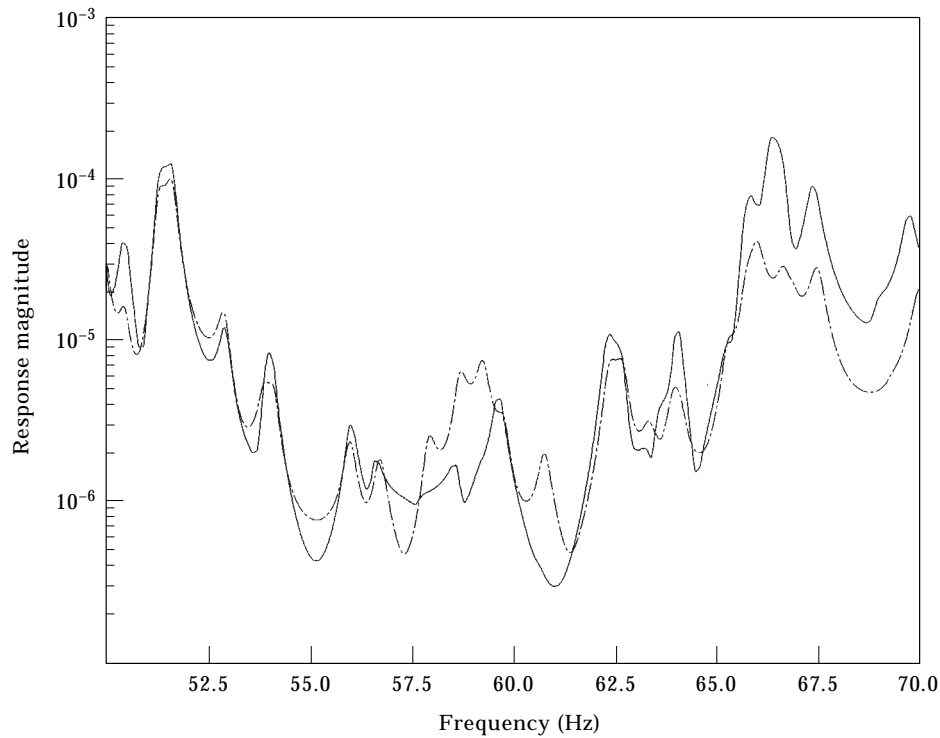
Figure 21. Response (deflection in m per unit force in N) of the spatially averaged and optimized mass-loaded, stepped plate, compared with results from the finite element method (ten 0·5 kg masses); key as per Figure 11.

the drive and response points used, as well as the range of frequencies considered, helps reduce this sensitivity [17]. The optimized design is then based on those mass positions that produce the minimum average objective function. Such spatial averaging does, however, result in somewhat reduced vibration isolation characteristics: this deterioration is traded off against the increased robustness of the results.

Here, spatial averaging was carried out on the stepped plate carrying 10 point masses. The unit harmonic force was applied at three different points on the first bay, forming the corners of an equilateral triangle. The sides of the triangle were one quarter of the wave length of the mid-frequency (60 Hz) in length, which is about 0·1 m. On the fifth bay, seven different response points were then chosen, forming the corners and centre of a hexagon with similar length sides. Six random combinations of these possible input–output points were chosen and the corresponding responses calculated, from which the average response was obtained. The GA optimization process was carried out aiming to minimize the integral of the average response within the frequency range of 55–65 Hz. Figure 19 shows the resulting optimized mass positions together with the original random positions. The response of the plate for these optimized mass positions is plotted in Figures 20 and 21 where it is compared with the average responses for random mass positions, the unloaded plate and an equivalent FE model (cf. Figures 14 and 15). Again, significant reductions in energy transfer over the frequency range of interest are achieved and, moreover, correlation with the FE results is improved. The spaced averaged optimized objective function for the mass-loaded plate was found to be 12·78 times less than for the unloaded plate. As expected, this reduction is rather less than that for single drive and response

points but still represents an order of magnitude increase in noise isolation over the bare stiffened plate. It is also more likely to be realisable in practice.

8. CONCLUSIONS

An existing analytical method has been developed to deal with the vibrational behaviour of simply supported stepped plates. Comparisons of this approach with the dynamic stiffness and finite element methods reveal almost perfect agreement. Having established the validity of the method, it has then been combined with the method of FDF to tackle the vibration analysis of a mass-loaded stepped plate. Numerical examples of various configurations have been compared with finite element models and satisfactory agreement obtained. This agreement is almost perfect with few added masses but starts to deteriorate as the number of masses rises. The main characteristic of the method presented are: (a) the method is analytically based and allows direct control over the parameters determining the vibrational behaviour of mass-loaded stepped plates; (b) it is easy to implement being based on simple underlying equations and (c) the speed of solution is very much faster than using equivalent finite element methods. These characteristics make the approach ideal for the ultimate aim of this work which is the vibrational optimization of mass-loaded stepped plates.

The objective function used here is taken to be minimization of the integral of the response of a mass-loaded stepped plate over a limited band of frequencies containing some 10–15 modes. The GA, which is an evolutionary computing method, has been employed to search for suitable mass positions in order to minimize this objective. The results from using various numbers of masses (while keeping the overall added mass constant) show that significant reductions in vibration transmission can be obtained. The results also indicate that, with the same overall mass value, greater reductions in the objective function are achieved by using increased numbers of smaller point masses scattered on the plate. Finally, to enhance the robustness of the resulting designs, the optimization process for the 10 mass cases has been carried out using spatial averaging of the drive and response points. This final approach improves correlation of the results with the finite element models.

It is hoped that the work presented demonstrates that significant passive structural vibration control might be achieved in real structures by accepting modest departures from conventional plated and stiffened designs.

ACKNOWLEDGMENT

REFERENCES

1. R. S. LANGLEY 1989 *Journal of Sound and Vibration* **135**, 319–331. Application of the dynamic stiffness method to the free and forced vibrations of aircraft panels.
2. A. J. KEANE 1994 in *I. C. PARMEE* (ed.) *Proceedings of the Conference on Adaptive Computing in Engineering Design and Control* 94, *Plymouth*, *P.E.D.C.*, 14–27. Experiences with optimizers in structural design.
3. D. J. MEAD 1975 *Journal of Sound and Vibration* **40**(1), 1–18. Wave propagation and natural modes in periodic systems: I. Mono-coupled systems.
4. D. J. MEAD 1975 *Journal of Sound and Vibration* **40**(1), 19–39. Wave propagation and natural modes in periodic systems: I. Multi-coupled systems, with and without damping.

5. S. J. Guo, A. J. Keane and M. Moshrefi-Torbati 1997 *Journal of Sound and Vibration* **204**(4), 645–657. Vibration analysis of stepped thickness plates.
6. I. Chopra 1997 *International Journal of Mechanical Sciences* **16**, 337–344. Vibration of stepped thickness plates.
7. S. Kirkpatrick, C. D. Gelatt Jr. and M. P. Vecchi 1983 *Science* **220**(4598), 671–680. Optimization by simulated annealing.
8. D. E. Goldberg 1989 *Genetic Algorithms in Search, Optimization and Machine Learning*. Reading, MA: Addison–Wesley.
9. D. B. Fogel 1993 *Cybernetics and Systems* **24**(1), 27–36. Applying evolutionary programming to selected travelling salesman problems.
10. A. J. Keane 1993 in R. F. Albrecht, C. R. Reeves and N. C. Steele (eds.) *Proceedings of the International Conference on Artificial Neural Nets and Genetic Algorithms*. Innsbruck: Springer. pp. 536–543. Structural design for enhanced noise performance using Genetic Algorithm and other optimization techniques.
11. A. J. Keane 1995 *Artificial Intelligence in Engineering* **9**(2), 75–83. Genetic algorithm optimization of multi-peak problems: studies in convergence and robustness.
12. M. R. Anderberg 1975 *Cluster Analysis for Applications*. New York: Academic Press.
13. X. Yin and N. Germay 1993 in R. F. Albrecht, C. R. Reeves and N. C. Steele (eds.) *Proceedings of the International Conference on Artificial Neural Nets and Genetic Algorithms*. Innsbruck: Springer. pp. 450–457. A fast genetic algorithm with sharing scheme using cluster methods in multimodal function optimization.
14. R. E. D. Bishop and D. C. Johnson 1960 *The Mechanics of Vibration*. Cambridge: Cambridge University Press.
15. I-DEAS Master Series Reference Manual. S.D.R.C. 1994.
16. A. J. McMillan and A. J. Keane 1996 *Journal of Sound and Vibration* **192**(20), 549–562. Shifting resonances from a frequency band by applying concentrated masses to a thin rectangular plate.
17. A. J. Keane and A. P. Bright 1996 *Journal of Sound and Vibration* **190**(4), 713–719. Passive vibration control via unusual geometries: experiments on model aerospace structures.

NOTATION

a, b	plate dimensions
N	number of plate subsections
h_i	thickness of the ith part of the plate
A_n, B_n, C_n, D_n	coefficients of the shape functions
D	plate flexural rigidity, $Eh^3/12(1 - v^2)$
E	Young's Modulus
ρ	plate density
v	Poisson's ratio
α	$n\pi/b$
ω	frequency (rad/s)
k_i^4	$\rho\omega^2 h_i/D_i$
m	number of half sine waves in the x-direction
n	number of half sine waves in the y-direction
l	number of added masses
$w(x, y, t)$	time dependent transverse deflection of the plate
$W_j(x, y)$	shape function of the jth part of the plate
λ	eigenvalue
η	damping ratio
$\psi(x)$	shape function in the x-direction